

***Design, synthesis, optimization and antiviral activity of a class of hybrid dengue virus E protein inhibitors***

<sup>a</sup>Surender Singh Jadav<sup>°</sup>, <sup>b</sup>Suzanne Kaptein<sup>°</sup>, <sup>a</sup>Timiri Ajaykumar, <sup>b</sup>Tine De Burghgraeve, <sup>a</sup>Vishnu Nayak, <sup>a</sup>Ramesh Ganesan, <sup>a</sup>Barij Nayan Sinha, <sup>b,\*</sup>Johan Neyts, <sup>b</sup>Pieter Leyssen, <sup>a,\*</sup>Venkatesan Jayaprakash

<sup>a</sup>*Department of Pharmaceutical Sciences and Technology, Birla Institute of Technology, Mesra-835 215 (JH), India*

<sup>b</sup>*Laboratory for Virology and Experimental Chemotherapy, Rega Institute for Medical Research, University of Leuven (KU Leuven), B-3000 Leuven, Belgium*

<sup>°</sup>Both authors equally contributed to this work.

\*Corresponding author:

Venkatesan Jayaprakash

Department of Pharmaceutical Sciences, Birla Institute of Technology, Mesra-835215, India

Tel: +91-9470137264

E-mail: [venkatesanj@bitmesra.ac.in](mailto:venkatesanj@bitmesra.ac.in)

Johan Neyts

Rega Institute for Medical Research, University of Leuven (KU Leuven), B-3000 Leuven, Belgium

Tel: 0032-16-337353

E-mail: [Johan.Neyts@rega.kuleuven.be](mailto:Johan.Neyts@rega.kuleuven.be)

## **Abstract**

The  $\beta$ -OG pocket is a cavity in the flavivirus envelope (E) protein that was identified by Modis et al. (2003) as a promising site for the design of antiviral agents that interfere with virus entry into the host cell. The availability of the X-ray crystal structure of the dengue virus (DENV) E protein provided an opportunity for *in silico* drug design efforts to identify candidate inhibitors. The present study was set up to explore whether it is possible to generate a novel class of molecules that are hybrids between two hit compounds that have been reported previously by Zhou et al. (2008) following an *in silico* screening effort against the DENV E protein. First, a library of twenty hybrid molecules were designed and synthesized to explore the feasibility of this strategy. Antiviral evaluation in a virus-cell-based assay for DENV proved this approach to be successful, after which another twenty-four molecules were produced to further explore and optimize the potency of this novel class of hybrid inhibitors. In the end, a molecule was obtained with an  $EC_{50}$  against dengue virus serotype 2 in the low micromolar range (**23**,  $1.32 \pm 0.41 \mu\text{M}$ ).

**Keywords:** Dengue virus, E protein, pyrazolines, thiazoles, Schiff's bases

Dengue fever is a mosquito-transmitted viral disease that in the past decades has become endemic in most, if not all, tropical and sub-tropical regions around the world. Yearly, an estimated 50 to 200 million infections are caused by dengue virus (DENV),<sup>1</sup> with a fatal outcome in over 2.5% of the cases.<sup>2</sup> Globalization and climate change are drivers that continue to increase the impact of this infectious disease on human health.<sup>3</sup> The pharmaceutical industry is heavily investing in the development of an efficient vaccine, which until now still has failed to fulfill its promise.<sup>4</sup> Several antiviral drugs for the treatment or prevention of DENV infections are in the (pre)clinical stage, but it will take several more years before the first one will reach the clinic. [ENREF 5](#) In this latter context, any stage in the viral replication cycle may represent a possible target for the development of such small-molecule inhibitors.<sup>5-7</sup>

In 2003, Modis and colleagues reported the crystal structure of the DENV envelope (E) protein (1OKE).<sup>8</sup> In this structure, a density was observed that could be attributed to an n-octyl- $\beta$ -D-glucoside ( $\beta$ -OG) molecule, a detergent that is commonly used for the production of protein crystals. The cavity in the E protein in which this molecule fits, also designated the  $\beta$ -OG pocket, quickly drew the attention for structure-based drug screening and design efforts, especially because it was shown that fusion of the virus envelope with host cell membranes requires a pronounced conformational change of the E-protein as well as this cavity.<sup>9,10</sup> In this context, it was put forward that freezing the E protein in its pre-fusion state by filling the  $\beta$ -OG pocket with a small molecule would prevent virus fusion and thus would offer a novel and promising strategy for the development of a drug for the treatment or prevention of DENV infections.

In 2008, Zhou and colleagues performed a large-scale *in silico* screen from which the 23 top-ranking compounds were selected for evaluation in a yellow fever virus (YFV) assay as alternative for DENV.<sup>11</sup> Several compounds showed inhibitory activity, by which they validated this novel drug discovery approach. The purpose of the present study is to explore whether a novel hybrid chemical scaffold with more potent antiviral activity against DENV can be developed based on compounds M02 and D03 that have been reported in the aforementioned study (**Figure 1**). Even though these compounds

were shown to only have inhibitory activity in the higher micromolar range in the YFV assay (M02:  $IC_{50}=51\pm7\ \mu M$  & D03:  $IC_{50}=31\pm0.3\ \mu M$ , respectively), because YFV and DENV have a ~43.8% sequence identity at the amino acid level of the E protein (and even higher for the amino acids that line the  $\beta$ -OG pocket),<sup>12</sup> it was envisaged that compounds with similar or even a more potent inhibitory effect against DENV could be obtained. A similar approach was reported by Li et al. (2008),<sup>13</sup> which yielded methyl-4-(dibromomethyl)-2-(4-chlorophenyl)thiazole-5-carboxylate, a compound that later was developed into a metabolically more stable analogue by Mayhoub et al. (2011).<sup>14</sup> Few more reports on the identification of fusion inhibitors through High-Throughput Virtual Screening (HTVS) are available.<sup>12, 15-17</sup> [ENREF 10](#)

So far, all inhibitors of DENV infection that target the  $\beta$ -OG pocket have not been further developed. However, novel compound series undoubtedly will contribute to a better understanding of this pocket as target for small-molecule inhibitors.

A first series of twenty compounds (**1-20**, **Table 1**) was designed as hybrid molecules by grafting half of the structure of compound M02 onto half of the structure of compound D03 (see Zhou et al., 2008) (**Figure 1**). The resulting pyrazoline derivatives (**1-20**) were synthesized through the reactions outlined in **Scheme 1A**.<sup>18</sup> The synthesis starts with the preparation of chalcones from appropriate benzaldehydes and acetophenones in the presence of sodium hydroxide (60%) using methanol as solvent at room temperature for a period of 48 h. The resulting chalcones were converted into the respective pyrazolines by the reaction of thiosemicarbazide in the presence of sodium hydroxide under reflux using methanol as solvent for a period of 8-10 h. The final compounds (**1-20**) are obtained by the reaction of appropriate pyrazolines with either p-chloro phenacyl bromide or p-phenyl phenacyl bromide under reflux using ethanol as solvent for a period of 30-45 min.

None of the twenty molecules were able to inhibit the development of virus-induced cytopathic effects (CPE, virus-induced cell death) when compound and virus were added to the cells at the same time. However, when virus and compound were mixed and pre-incubated for 2 h at 37 °C, four compounds (**9**, **13**, **19**, **20**) showed antiviral activity. Based on only these four active compounds in

the library of pyrazolines (**1-20**), it was not feasible to deduct a detailed structure-activity relationship. However, useful information could be derived to devise further strategies for lead optimization. For example, the substitutions 4-biphenyl thiazol-2-yl, 4-methoxyphenyl and 3-methoxy-4-hydroxyphenyl at N1, 3<sup>rd</sup> and 5<sup>th</sup> position of the pyrazoline, respectively, appear to be favorable for antiviral activity. Compound **19** (EC<sub>50</sub>: 3.79 ± 1.22 µM, Table 3) was found to be the most potent amongst the twenty compounds.

Encouraged by and based on the results that were obtained with compounds **1-20**, compounds **21-44** (**Table 1**) were designed as open ring analogues of the hybrid scaffold with 7C-minus (phenyl ring at 5<sup>th</sup> position of pyrazoline and C5 of pyrazoline; **21-25**, **33-38**) and 8C-minus (phenyl ring at 5<sup>th</sup> position of pyrazoline and C4-C5 of pyrazoline; **26-32**, **39-44**) (**Figure 1**). This is consistent with the observation made by *Li et al.*: through simulation studies, they proposed that 5-aryl substitutions on the pyrazole moiety prevented the chlorophenyl thiazole part of the molecule to be completely embedded in the hydrophobic pocket.<sup>13</sup> All hydrazones were synthesized through reactions outlined in **Scheme 1B**.<sup>18-20</sup> The synthesis starts with the preparation of thiosemicarbazones of appropriate benzaldehyde and acetophenones in the presence of catalytic amount of glacial acetic acid using methanol as solvent. The reaction was carried out in room temperature for about 2 h. The final compounds (**21-44**) were prepared through the reaction of thiosemicarbazones with appropriate phenacyl bromide (p-chloro phenacyl bromide, p-phenyl phenacyl bromide) in methanol under room temperature, with stirring for about 30-60 minutes.

From the collection of thiazolyl hydrazones (**21-44**), five compounds (**23**, **36**, **37**, **39**, **41**) were shown to elicit an antiviral effect in the DENV assay in which the compounds were pre-incubated with the virus. These results indicate that the benzaldehyde hydrazones of 4-biphenyl thiazole-2-hydrazides (**39**, **41**) and acetophenone hydrazone of 4-chlorophenyl thiazole-2-hydrazide (**23**) are essential for antiviral activity. From this series, in particular compound **23** markedly inhibited DENV-induced cell death with the best selectivity index of all compounds (EC<sub>50</sub>: 5.8 ± 1 µM; CC<sub>50</sub>: 145.2 ± 12; SI: 25, **Table 2**, **Figure 2**). Due to the stringency of the virus-cell-based screening assay, only compounds that

have a clear antiviral effect produce an  $EC_{50}$  value, which explains that only few were found to have a cell protective effect.

For each of the nine compounds that showed activity in the CPE reduction assay, the antiviral activity was validated by quantification of the dose-response effect on the amount of dengue virus RNA that is produced by virus-infected, compound-treated cells (**Table 3**). For all nine compounds, an inhibitory effect was also observed in this assay, which for most of the compounds was proportionate to the previously observed cell protective effect. The antiviral activity of the most potent compound, i.e. compound **23**, was further validated by quantification of the dose-response effect on the production of infectious dengue virus progeny. Compound **23** exhibited a pronounced dose-dependent inhibition of plaque formation ( $EC_{50} = 1.39 \pm 0.06 \mu\text{M}$ , **Figure 3**), which was similar to the inhibition of viral RNA synthesis as determined in the virus yield reduction assay ( $EC_{50} = 1.32 \pm 0.41 \mu\text{M}$ , **Table 3**). Based on its antiviral potency and selectivity in both assays, compound **23** will become the subject of a more detailed and elaborate virological study into its precise molecular mechanism of action.

Analysis of the compounds docked into the  $\beta$ -OG pocket shows similar binding modes for compounds **1-10**, for which the 4-chlorophenyl thiazolyl portion was found to partially occupy the hydrophobic pocket or to be placed at the surface. For compound **11-20**, the biphenyl thiazolyl portion is well accommodated in the hydrophobic pocket, and three compounds (**13**, **19**, **20**) were found to be active. In case of compounds **21-44**, the 4-chlorophenyl thiazolyl and biphenyl thiazolyl portions were accommodated in variable positions into the hydrophobic pocket, which is predominantly determined by the nature and substitution(s) on the head group (pyrazoline and hydrazone portion). **Figure 4A** shows the interaction of compound **23** within the E protein of DENV. Van der Waals interactions predominate and there is an H-bonding interaction between the side chain carbonyl oxygen of THR280 and the hydrogen of thiazole N-H of compound **23**. The side chain methyl group of compound **23** engages into a strong hydrophobic interaction with the side chain of ILE270 and LEU277. The 4-chlorophenyl ring at the 4<sup>th</sup> position of the thiazole engages into a  $\pi$ - $\pi$  staking

interaction with PHE193 and PHE279, and hydrophobic interaction with LEU207. The 3,4-dichlorophenyl portion of MO2 and 4-chlorophenyl portion of DO3 were reported to exhibit a strong hydrophobic interaction with LEU207, but no  $\pi$ - $\pi$  staking was reported.<sup>11</sup> It is this interaction that causes compound **23** to rank as the most potent amongst the nine actives. Compound **29** lacks the side chain methyl group that overlaps with compound **23** at the 4-chlorophenyl thiazole portion. Furthermore, due to a slight deviation of the head group (which is positioned near the surface), the hydrophobic interaction with either ILE270 or LEU277 cannot be established. While compound **3** can be seen as a cyclic precursor, it cannot insert its 4-chlorophenyl thiazole portion into the hydrophobic pocket (**Figure 4A**, 2D-plots are provided in the Supplementary material). Analysis of compound **13**, **35** and **41** showed that only compound **41** could position its biphenyl portion in such a way that it establishes the favorable  $\pi$ - $\pi$  staking with PHE193 and PHE279. This explains why this molecule is more potent than its cyclic counterpart **13**. Compound **35**, which differs from **41** only by one methyl group, incompletely occupies the hydrophobic pocket while the head portion is largely exposed to the solvent. This explains the inactivity of this molecule (**Figure 4B**, 2D-plots are provided in Supplementary material). As to what concerns compounds **19**, **36** and **42**; compound **19** establishes hydrophobic interactions and  $\pi$ - $\pi$  stacking in the hydrophobic pocket as well as H-bonding interaction (GLN200, LYS202) and  $\pi$ -cation interaction (LYS47) near the surface. This renders this compound more potent than compound **36**, its open ring counterpart. Compound **42**, which differs from compound **36** by one methyl group, can be freely accommodated by the cavity but is not able to establish a  $\pi$ - $\pi$  interaction with either PHE193 or PHE297 (**Figure 4C**, 2D-plot are provided in Supplementary material). In summary, the following interactions at the hydrophobic pocket are essential for antiviral activity: (i) the  $\pi$ - $\pi$  interaction with either PHE193 or PHE297, (ii) hydrophobic interaction with LEU207, and (iii) interactions at the surface by (a) a hydrophobic interaction with either ILE270 or LEU277 and (b) H-bonding interaction. The best molecule should establish H-bonding interaction near the surface, which helps in anchoring the molecule at the entrance (surface),

thereby facilitating the tail portion (4-chlorophenyl or biphenyl portion) to be accommodated in the hydrophobic pocket, while establishing the  $\pi$ - $\pi$  interaction.

## Acknowledgement

The authors acknowledge AICTE, GoI, India for JRF. Central Instrumentation Facility, BIT, Mesra and Dr. Reddy's Institute of Life Sciences, Hyderabad are acknowledged for Spectral Characterization of Samples. We also would like to thank Mieke Flament and Ruben Pholien for their excellent assistance with the generation of the virus yield and plaque reduction assay data.

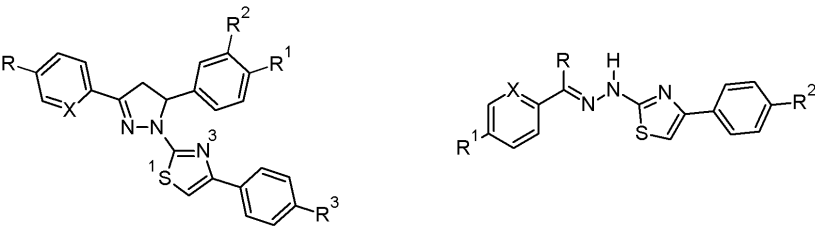
## References

1. Murray, N.; Quam, M. B.; Wilder-Smith, A. *Clinical epidemiology* **2012**, *5*, 299.
2. WHO. **2014**.
3. Ali, M. *Clinical epidemiology* **2013**, *5*, 461.
4. Yauch, L.; Shresta, S. *Advances in virus research* **2013**, *88*, 315.
5. Sampath, A.; Padmanabhan, R. *Antiviral Research* **2009**, *81*, 6.
6. Noble, C. G.; Chen, Y.-L.; Dong, H.; Gu, F.; Lim, S. P.; Schul, W.; Wang, Q.-Y.; Shi, P.-Y. *Antiviral Research* **2010**, *85*, 450.
7. Lim, S. P.; Wang, Q.-Y.; Noble, C. G.; Chen, Y.-L.; Dong, H.; Zou, B.; Yokokawa, F.; Nilar, S.; Smith, P.; Beer, D. *Antiviral research* **2013**, *100*, 500.
8. Modis, Y.; Ogata, S.; Clements, D.; Harrison, S. C. *Proc Natl Acad Sci U S A* **2003**, *100*, 6986.
9. Modis, Y.; Ogata, S.; Clements, D.; Harrison, S. C. *Nature* **2004**, *427*, 313.
10. Bressanelli, S.; Stiasny, K.; Allison, S. L.; Stura, E. A.; Duquerroy, S.; Lescar, J.; Heinz, F. X.; Rey, F. A. *The EMBO journal* **2004**, *23*, 728.
11. Zhou, Z.; Khaliq, M.; Suk, J. E.; Patkar, C.; Li, L.; Kuhn, R. J.; Post, C. B. *ACS Chem Biol* **2008**, *3*, 765.
12. Kampmann, T.; Yennamalli, R.; Campbell, P.; Stoermer, M. J.; Fairlie, D. P.; Kobe, B.; Young, P. R. *Antiviral Res* **2009**, *84*, 234.
13. Li, Z.; Khaliq, M.; Zhou, Z.; Post, C. B.; Kuhn, R. J.; Cushman, M. *J Med Chem* **2008**, *51*, 4660.
14. Mayhoub, A. S.; Khaliq, M.; Kuhn, R. J.; Cushman, M. *J Med Chem* **2011**, *54*, 1704.
15. Wang, Q. Y.; Patel, S. J.; Vangrevelinghe, E.; Xu, H. Y.; Rao, R.; Jaber, D.; Schul, W.; Gu, F.; Heudi, O.; Ma, N. L.; Poh, M. K.; Phong, W. Y.; Keller, T. H.; Jacoby, E.; Vasudevan, S. G. *Antimicrob Agents Chemother* **2009**, *53*, 1823.
16. Poh, M. K.; Yip, A.; Zhang, S.; Priestle, J. P.; Ma, N. L.; Smit, J. M.; Wilschut, J.; Shi, P. Y.; Wenk, M. R.; Schul, W. *Antiviral Res* **2009**, *84*, 260.
17. Yennamalli, R.; Subbarao, N.; Kampmann, T.; McGeary, R. P.; Young, P. R.; Kobe, B. *J Comput Aided Mol Des* **2009**, *23*, 333.
18. El-Sabbagh, O. I.; Baraka, M. M.; Ibrahim, S. M.; Pannecouque, C.; Andrei, G.; Snoeck, R.; Balzarini, J.; Rashad, A. A. *Eur J Med Chem* **2009**, *44*, 3746.
19. Turan-Zitouni, G.; Chevallet, P.; Kiliç, F. S.; Erol, K. *Eur J Med Chem* **2000**, *35*, 635.
20. Turan-Zitouni, G.; Ozdemir, A.; Kaplancikli, Z. A.; Benkli, K.; Chevallet, P.; Akalin, G. *Eur J Med Chem* **2008**, *43*, 981.

Note: Refer Supplementary material for synthetic procedures, spectral characterization and biological characterization



Table 1. Structural formulas of compounds 1-44



1-20						21-44					
Code	X	R	R <sup>1</sup>	R <sup>2</sup>	R <sup>3</sup>	Code	X	R	R <sup>1</sup>	R <sup>2</sup>	R <sup>3</sup>
1	CH	-H	-H	-H	-Cl	23	CH	-CH <sub>3</sub>	-OH	-Cl	-
2	CH	-Cl	-H	-H	-Cl	24	CH	-CH <sub>3</sub>	-OCH <sub>3</sub>	-Cl	-
3	CH	-OH	-H	-H	-Cl	25	CH	-CH <sub>3</sub>	-NO <sub>2</sub>	-Cl	-
4	CH	-OCH <sub>3</sub>	-H	-H	-Cl	26	N	-CH <sub>3</sub>	-H	-Cl	-
5	CH	-NO <sub>2</sub>	-H	-H	-Cl	27	CH	-H	-H	-Cl	-
6	N	-H	-H	-H	-Cl	28	CH	-H	-Cl	-Cl	-
7	CH	-Cl	-OH	-OCH <sub>3</sub>	-Cl	29	CH	-H	-OH	-Cl	-
8	CH	-Cl	-OH	-H	-Cl	30	CH	-H	-OCH <sub>3</sub>	-Cl	-
9	CH	- OCH <sub>3</sub>	-OH	-OCH <sub>3</sub>	-Cl	31	CH	-H	-NO <sub>2</sub>	-Cl	-
10	CH	- OCH <sub>3</sub>	-OH	-H	-Cl	32	N	-H	-H	-Cl	-
11	CH	-H	-H	-H	-C <sub>6</sub> H <sub>5</sub>	33	CH	-CH <sub>3</sub>	-H	-C <sub>6</sub> H <sub>5</sub>	-
12	CH	-Cl	-H	-H	-C <sub>6</sub> H <sub>5</sub>	34	CH	-CH <sub>3</sub>	-Cl	-C <sub>6</sub> H <sub>5</sub>	-
13	CH	-OH	-H	-H	-C <sub>6</sub> H <sub>5</sub>	35	CH	-CH <sub>3</sub>	-OH	-C <sub>6</sub> H <sub>5</sub>	-
14	CH	-OCH <sub>3</sub>	-H	-H	-C <sub>6</sub> H <sub>5</sub>	36	CH	-CH <sub>3</sub>	-OCH <sub>3</sub>	-C <sub>6</sub> H <sub>5</sub>	-
15	CH	-NO <sub>2</sub>	-H	-H	-C <sub>6</sub> H <sub>5</sub>	37	CH	-CH <sub>3</sub>	-NO <sub>2</sub>	-C <sub>6</sub> H <sub>5</sub>	-
16	N	-H	-H	-H	-C <sub>6</sub> H <sub>5</sub>	38	N	-CH <sub>3</sub>	-H	-C <sub>6</sub> H <sub>5</sub>	-
17	CH	-Cl	-OH	-OCH <sub>3</sub>	-C <sub>6</sub> H <sub>5</sub>	39	CH	-H	-H	-C <sub>6</sub> H <sub>5</sub>	-
18	CH	-Cl	-OH	-H	-C <sub>6</sub> H <sub>5</sub>	40	CH	-H	-Cl	-C <sub>6</sub> H <sub>5</sub>	-
19	CH	- OCH <sub>3</sub>	-OH	-OCH <sub>3</sub>	-C <sub>6</sub> H <sub>5</sub>	41	CH	-H	-OH	-C <sub>6</sub> H <sub>5</sub>	-
20	CH	- OCH <sub>3</sub>	-OH	-H	-C <sub>6</sub> H <sub>5</sub>	42	CH	-H	-OCH <sub>3</sub>	-C <sub>6</sub> H <sub>5</sub>	-
21	CH	-CH <sub>3</sub>	-H	-Cl	-	43	CH	-H	-NO <sub>2</sub>	-C <sub>6</sub> H <sub>5</sub>	-
22	CH	-CH <sub>3</sub>	-Cl	-Cl	-	44	N	-H	-H	-C <sub>6</sub> H <sub>5</sub>	-

**Table 2.** Antiviral activity against DENV-2 as determined in a CPE-reduction assay

Compound	EC <sub>50</sub> (μM)	CC <sub>50</sub> (μM)	SI
9	0.79	2.4	3
13	13.2	79.2	6
19	8.4 ± 2.5	16.8 ± 4.1	2
20	24.8	> 99	> 4
23	5.8 ± 1.2	145 ± 12	25
36	100 ± 9	200 ± 11	2
37	41 ± 5	82 ± 7	2
39	35.2	> 141	> 4
41	16.8	> 135	> 8

Values expressed in μM. Compound and virus was pre-incubated for 2 hours. For all other compounds, no antiviral activity has been observed (data not shown).

**Table 3.** Antiviral activity against DENV-2 as determined in a virus yield reduction assay

Compound	EC <sub>50</sub> (μM)	CC <sub>50</sub> (μM)	SI
9	7.00 ± 4.16	54.6 ± 38.8	8
13	8.44 ± 2.02	86.8 ± 30.1	10
19	3.79 ± 1.22	25.6 ± 11.9	7
20	18.6 ± 5.50	99.3 ± 0.00	5
23	1.32 ± 0.41	125.0 ± 40.8	95
36	17.7 ± 4.50	116.8 ± 8.22	7
37	12.2 ± 1.14	70.8 ± 43.2	6
39	127.8 ± 29.9	> 141	> 1
41	5.29 ± 4.80	> 135	> 25
Ribavirin	47.9 ± 4.63	> 410	> 9

Values expressed in μM. Values represents averages of 3 independent experiments. For all other compounds, no such data were generated.

**Legends to scheme and figures**

**Scheme 1 Reagents and conditions A:** (a) MeOH, NaOH (60%), rt, 48 h; (b)  $\text{NH}_2\text{-CS-NH-NH}_2$ , MeOH, NaOH, reflux, 8-10 h; (c)  $\text{R}^3\text{-C}_6\text{H}_4\text{-CO-CH}_2\text{Br}$ , EtOH, reflux, 30-45 min. **B:** (a) MeOH,  $\text{NH}_2\text{-CS-NH-NH}_2$ , (AcOH glacial), rt, 2 h; (b) MeOH,  $\text{R}^2\text{-C}_6\text{H}_4\text{-CO-CH}_2\text{Br}$ , rt, 30-60 min stirring.

**Figure 1 Design of Library molecules (1-44).**

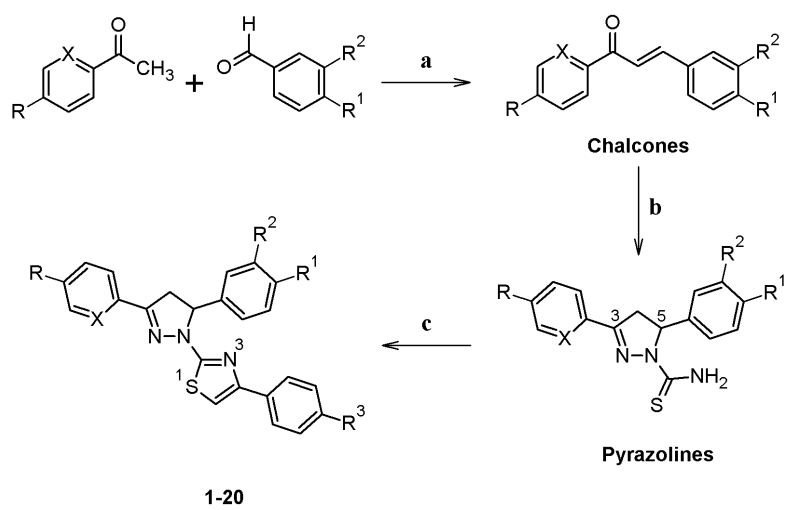
**Figure 2.** CPE reduction assay of compound **23** (Pre-incubation antiviral assay)

**Figure 3.** Dose-response effect of compound **23** on dengue virus serotype 2 plaque formation. The numbers of plaques were quantified on day 6 post-infection after fixation and staining

**Figure 4A.** Compounds **3** (Green), **23**(Blue), and **29** (Red) in BOG-pocket of DENV2 E-protein (PDB Code: 1OKE); **4B.** Compounds **13** (Green), **35** (Blue) and **41** (Red) in BOG-pocket of DENV2 E-protein (PDB Code: 1OKE); **4C.** Compounds **19** (Green), **36** (Blue) and **42** (Red) in BOG-pocket of DENV2 E-protein (PDB Code: 1OKE).

## Scheme 1

**A**



**B**

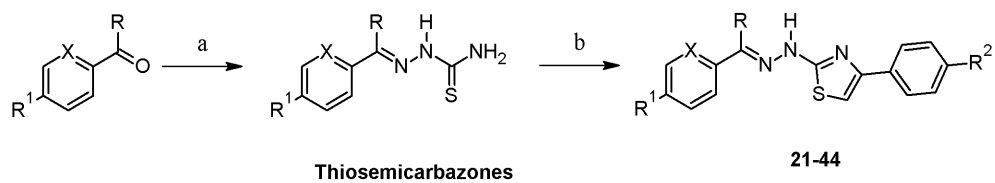


**Figure 1.**

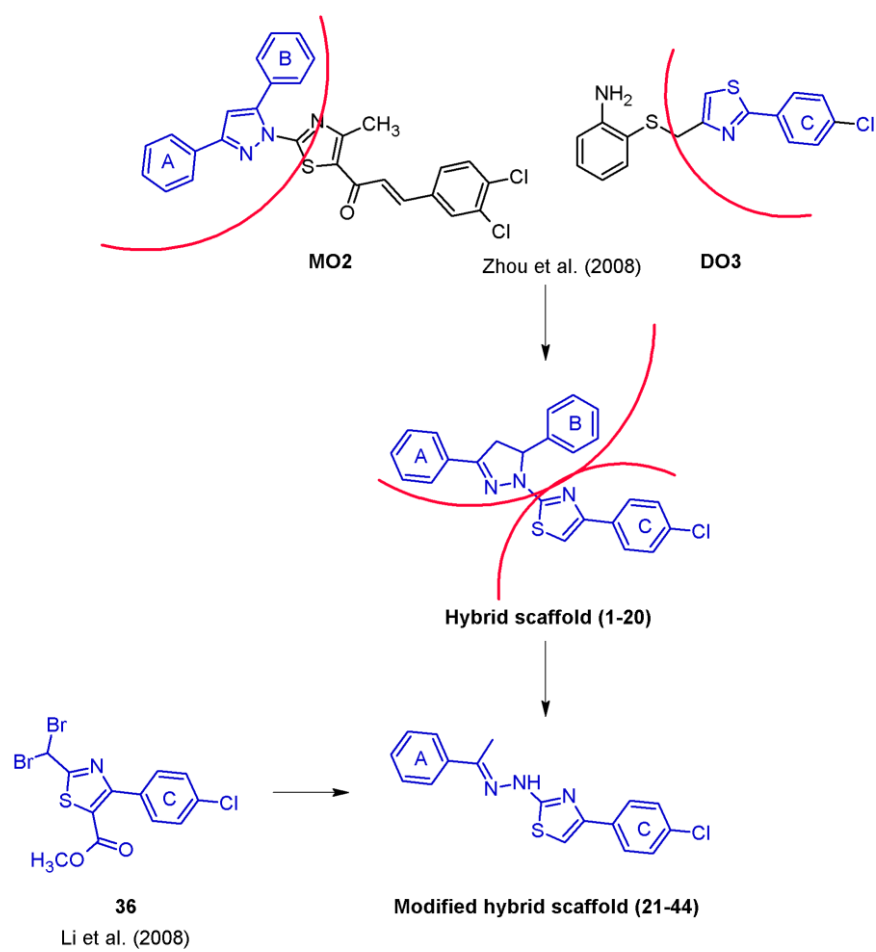


**Figure 2**

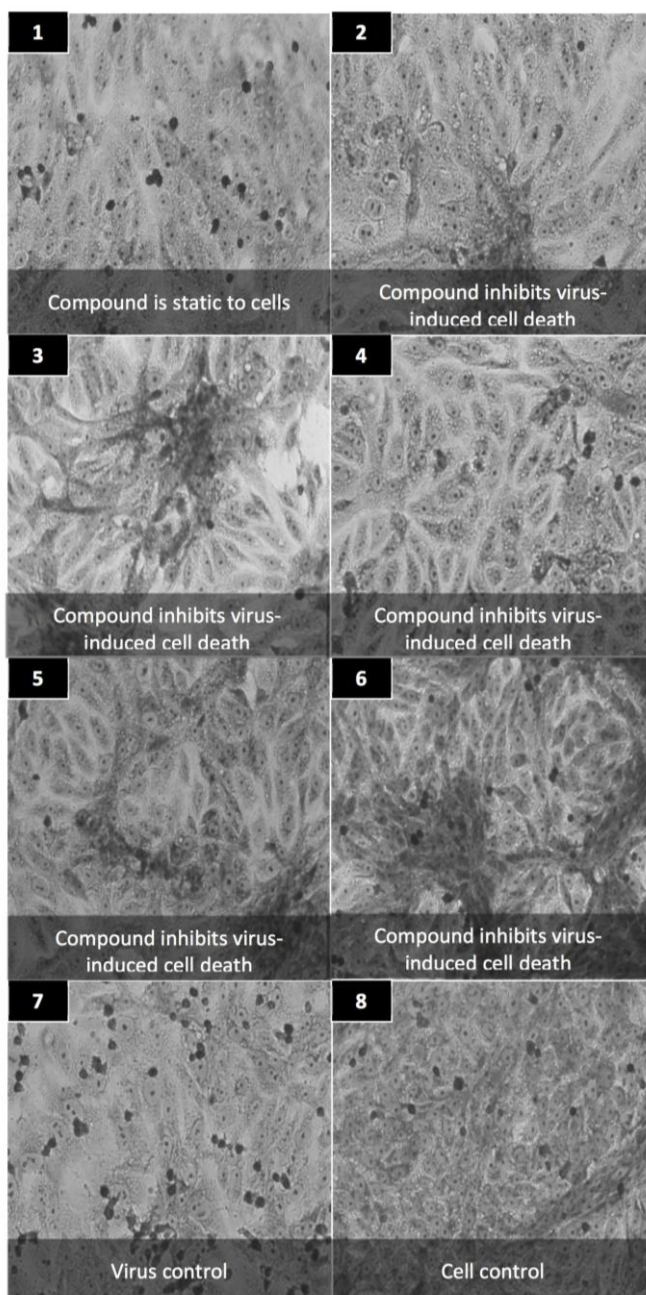


**Figure 3**

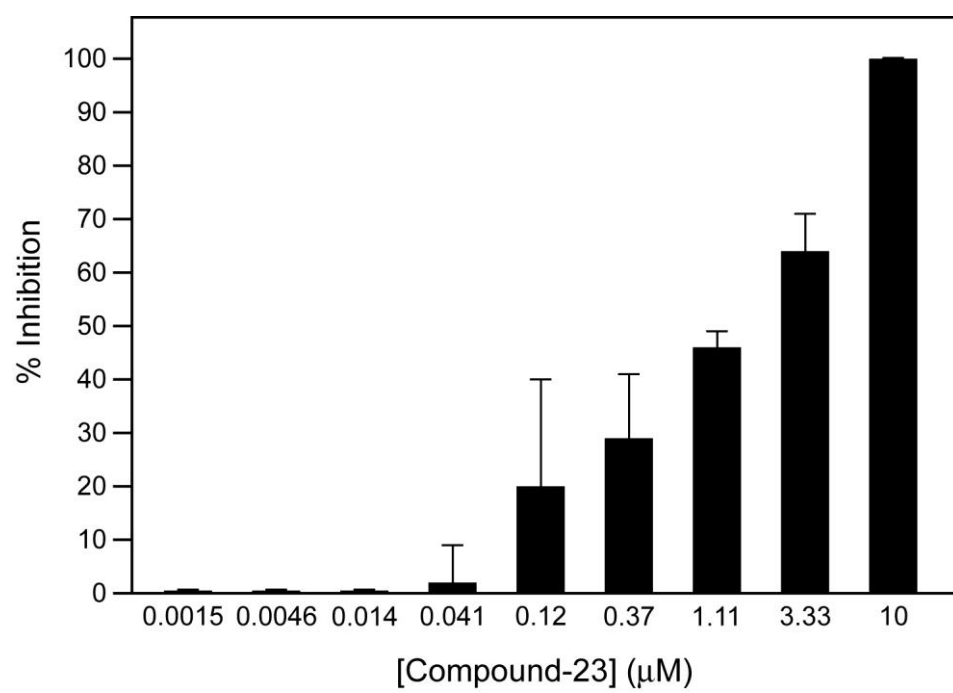


Figure 4A

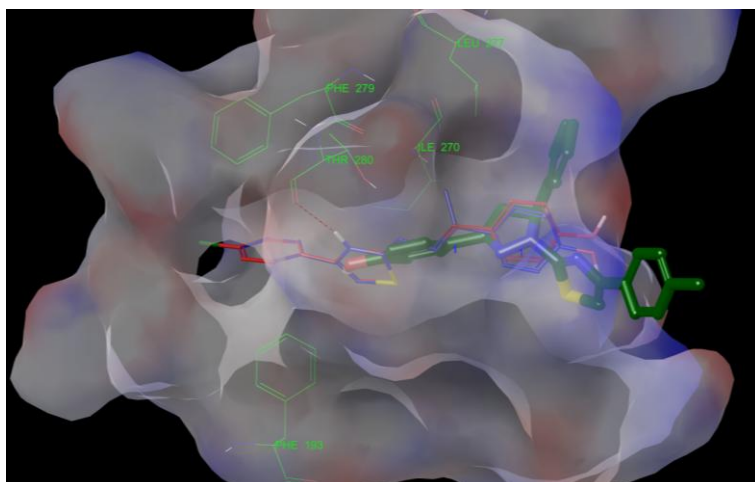


Figure 4B

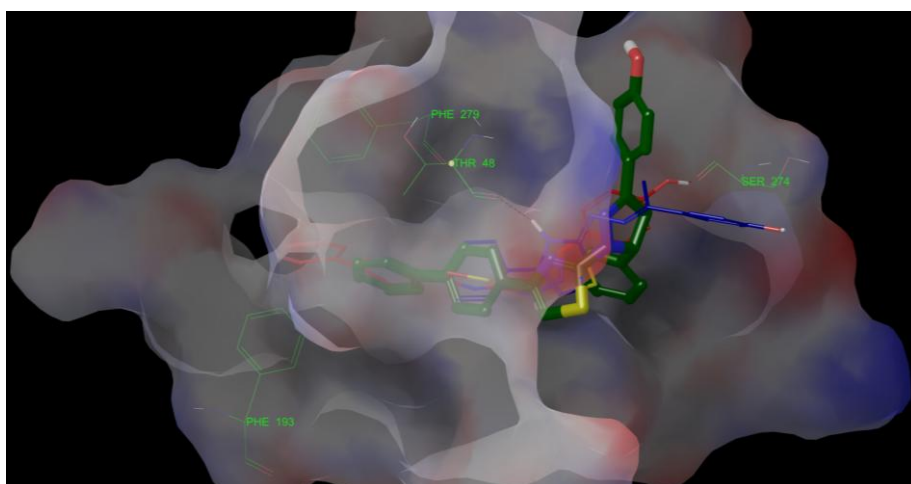
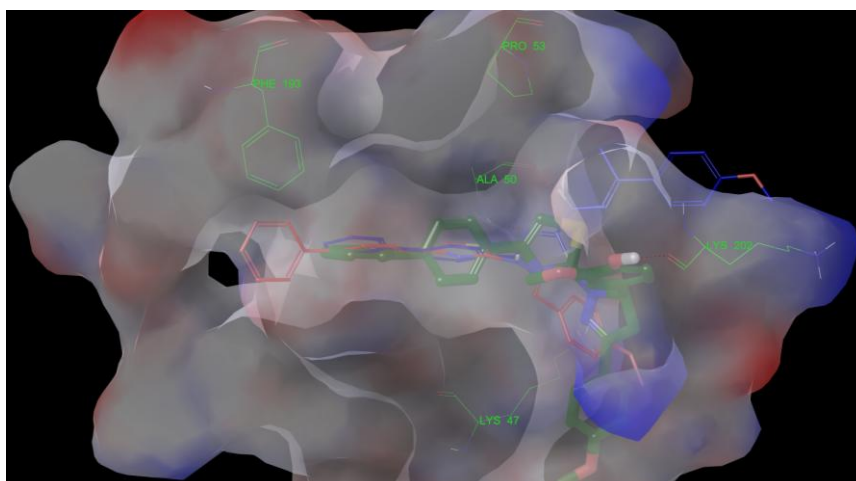


Figure 4C





## Supplementary Material

[Click here to download Supplementary Material: SupplimentaryMaterial.doc](#)